ELSEVIER

Contents lists available at ScienceDirect

Journal of Membrane Science

journal homepage: www.elsevier.com/locate/memsci



Self-cleaning membranes for water purification by co-deposition of photomobile 4,4'-azodianiline and bio-adhesive polydopamine



Sankara Narayanan Ramanan^a, Nima Shahkaramipour^a, Thien Tran^a, Lingxiang Zhu^a, Surendar R. Venna^b, Chang-Keun Lim^c, Ajay Singh^c, Paras N. Prasad^c, Haiqing Lin^a,*

- a Department of Chemical and Biological Engineering, University at Buffalo, The State University of New York, Buffalo, NY 14260, USA
- National Energy Technology Laboratory/AECOM, 626 Cochrans Mill Rd., Pittsburgh, PA 15236, USA
- ^c The Institute for Lasers, Photonics and Biophotonics, University at Buffalo, The State University of New York, Buffalo, NY 14260, USA

ARTICLE INFO

Keywords: Water purification Self-cleaning membranes Photoresponsive materials Azobenzene Polydopamine

ABSTRACT

Stimuli-responsive membranes have been widely explored to mitigate fouling on the membrane surface to achieve the stable performance of water purification. Herein, a facile one-step coating of photo-mobile materials on membrane surface was developed to impart self-cleaning property upon exposure alternatively to ultraviolet (UV) and visible light. Specifically, photo-mobile 4,4′-azodianiline (AZO) and a bio-adhesive polydopamine (PDA) were co-deposited on the surface of ultrafiltration (UF) membranes. The effect of the coating layer on the surface hydrophilicity and pure water permeance was systematically evaluated. The photoresponsive properties of AZO in solutions and thin films with PDA was characterized using UV–Vis absorption spectroscopy. When exposed with UV light, AZO undergoes photoisomerization from *trans*-AZO to *cis*-AZO, decreasing the volume, while the exposure to visible light enables the transition from the *cis*- to *trans*- configuration, increasing the volume. The resulted self-cleaning behavior of the modified membranes through the reversible volume change is demonstrated in treating 1 g/L bovine serum albumin (BSA) solution. After exposure to the alternative UV/vis light, the AZO-coated UF membranes showed an increased water permeance by ~160%.

1. Introduction

Membrane technology has emerged as an important approach for water purification and wastewater treatment due to its high energy-efficiency, compactness, and simplicity in operation [1–3]. One major challenge to membrane processes is fouling, where contaminants in the feed accumulate on the membrane surface or inside the pores of the membrane, decreasing water permeance and increasing operating costs [4–8]. Fouled membranes can be cleaned at regular intervals using chemicals (such as acids, bases, or biocides) or backflushing [9]. Such cleaning interrupts the operation, and the use of strong chemicals causes irreversible damage to the membrane surface and therefore reduces the service life of the membrane [10]. Fouling can also be mitigated by membrane surface modification, such as enhancing surface hydrophilicity [5,8], creating surface nanopatterns [11–13], and both [14].

Self-cleaning membranes comprising a thin layer of "smart" materials on the surface have been explored to mitigate fouling without the use of strong chemicals [15-18]. Such smart materials respond to the changes in their environment (e.g., pH [19-21], ionic strength [22],

magnetic field [23], temperature [24], and light [21,25–27]) causing changes in water flux and surface properties. Among the different kinds of stimuli, light is of special interest, as it can be easily controlled regarding time and space and also functions as a non-invasive stimulus [28]. In this approach, photoresponsive materials are grafted or coated on the membrane surface to provide switchable and antifouling properties [21,25–27]. For example, spiropyran-based materials become zwitterionic and thus more hydrophilic upon exposure to UV light [26,29], and the switchability can be used to generate the antifouling surface [26,27].

Azobenzene is photo-mobile since it can easily and quickly undergo photoisomerization between the *trans*- and *cis*- configuration [25]. As depicted in Fig. 1, the UV radiation leads to the transition from *trans*- to *cis*-configuration, which drastically decreases the distance between the *para* carbon atoms, from 9.9 Å to 5.5 Å, and increases the dipole moment, from 0.5 Debye (D) to 3.1 D [30,31]. The isomerization is reversible, and the *trans*-azobenzene forms when UV radiation is switched off. The photoisomerization also induces changes in the volume of azobenzene-containing materials. For instance, azobenzene-based liquid-crystalline elastomer films contracted by about 3% in length after

E-mail address: haiqingl@buffalo.edu (H. Lin).

^{*} Corresponding author.

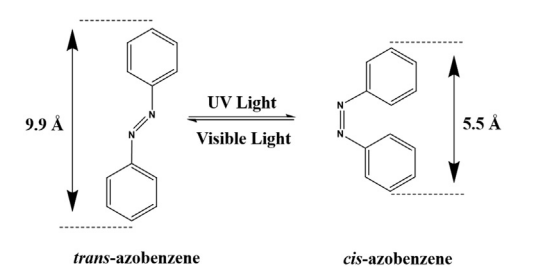


Fig. 1. Reversible photoisomerization and volume change of photo-mobile azobenzene [30].

exposure to UV light at 100 mW/cm² for 100 s [32]. The azobenzene-based derivatives have been used to modify the membrane surface to control the surface wettability and permeability using UV light [25,33–35]. However, the azobenzene groups are often chemically incorporated in polymers [34], which are very challenging to be deposited as a thin film on membranes without blocking the pores and significantly decreasing water permeance.

The objective of this study was to demonstrate a facile one-step coating of photo-mobile 4,4'-azodianiline (AZO) on commercial UF membranes to achieve self-cleaning behavior when exposed to UV light and visible light alternatively, as shown in Fig. 2. The AZO is co-deposited with dopamine in aqueous solution to form a stable thin film on different UF membranes. In the presence of oxygen, dopamine forms complexes (polydopamine or PDA) through $\pi\text{-}\pi$ stacking and hydrogen bonding [36–38]. The hydrophilic PDA is insoluble in water, and it has high adhesion properties, similar to the composition of adhesive proteins in mussels. More importantly, the PDA can be utilized to covalently graft amine-, acrylate- and thiol-containing compounds to the membrane surface through Michael addition or Schiff base reactions [6,39–41]. As shown in Fig. 2a, the amine-containing AZO can react with PDA through Michael addition, depositing on the solid portion of the membranes without dramatically blocking the surface pores. AZO may also interact with PDA through π - π stacking and hydrogen bonding (non-covalent bonds) [41-44]. Both the covalent and non-covalent bonding result in a photo-mobile, stable thin film on the membranes. The coating layer is hypothesized to be on the solid portion of the membranes without covering the pores.

Fig. 2b depicts the self-cleaning behavior of the PDA/AZO layer. By alternatively exposure to the UV/vis light, the PDA/AZO layer shrinks and expands reversibily, mitigating the aggregation of the foulants on

the membrane surface. Additionally, the PDA provides UV protection and free radical scavenging [45], which increases the membranes stability under UV light [45]. For instance, a self-protected, self-cleaning UF membrane, synthesized using the UV resilient property of PDA and the photocatalytic ability of TiO₂-NH₂, demonstrated consistent performance even after prolonged exposure to UV irradiation [46].

This work, for the first time, demonstrates the self-cleaning behavior of membranes derived from the coating layer of AZO and PDA on the membrane surface. The effect of the coating layer on the surface hydrophilicity and pure water permeance was systematically evaluated in this study. The photoresponsive properties of AZO in the solution and thin films with PDA was thoroughly characterized using UV–Vis absorption spectroscopy. The self-cleaning behavior of the coating layer on UF membranes was demonstrated by treating water containing bovine serum albumin (BSA). Because this facile one-step modification of membrane surface occurs in aqueous solution, it can be readily applied as post-modification for membranes and modules.

2. Experimental

2.1. Materials

Flat-sheet UF membranes of polysulfone (PSf) with molecular weight cutoff (MWCO) of 30 kDa, and polyvinylidene fluoride (PVDF) with MWCO of 250 kDa were obtained from Nanostone Water (Eden Prairie, MN). Polyethersulfone (PES) UF membranes with MWCO of 2 kDa were procured from Alfa Laval Inc. (Richmond, VA). Dopamine hydrochloride, PSf beads (M_n ~ 22,000), BSA (> 96%), cyclopentanone (> 99%), Trizma® base (> 99.9%), phosphate buffered saline (PBS) powder, and n-decane (> 99%) were purchased from Sigma Aldrich (St. Louis, MO). 4,4'-Azodianiline (95%) was purchased from Acros Organics (NJ). Ethanol (190 proof), methanol (> 99.8%) and N, N-dimethylformamide (DMF) (> 99.8%) were obtained from Decon Labs (King of Prussia, PA), VWR International (Radnor, PA), and Fisher Scientific (Fairlawn, NJ), respectively. Nitrogen with ultrahigh purity was purchased from Praxair Inc. (Tonawanda, NY). Deionized (DI) water was generated by Milli-Q water equipment (18.2 M Ω cm at 23 °C) (EMD Millipore, Billerica, MA).

2.2. Membrane pretreatment and surface modification

Commercial UF membranes were pre-treated by soaking in ethanol and then in DI water for 24h each to remove pore-preserving agents

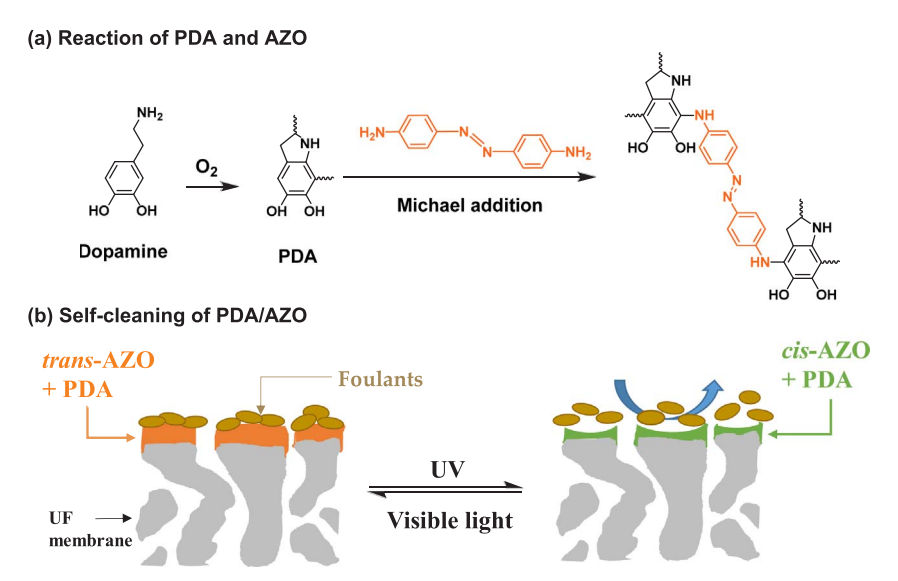


Fig. 2. (a) Scheme of PDA formation and reactions between AZO and PDA through Michael addition, leading to covalent linkages [41], and (b) schematic of the self-cleaning behavior of a photoresponsive membrane comprising a thin film of AZO and PDA.

such as glycerin following the procedure described in the literature [44].

For the membrane surface modification, the pre-treated membrane was attached to a plate and gasket assembly with the active side of the membrane facing upwards. The membrane coating assembly was placed on top of a rocking platform (VWR International, Radnor, PA). The rocker allows the membrane surface to be exposed to the oxygen in the air for dopamine polymerization [41]. A desired amount of AZO and dopamine was dissolved in a water-methanol mixture containing 70 vol% methanol. Trizma* base was added to the solution to obtain a pH of 8.5 to enable the polymerization of dopamine [41]. After coating for a desired time (0.5, 1, or 2 h), the modified membrane was rinsed with the DI water thoroughly to remove any unreacted chemicals and then stored in the DI water. The coating condition is denoted as *x*-PDA/*y*-AZO-zh, where *x* and *y* represent the concentration (g/L) of PDA and AZO in the coating solution, respectively, and *z* represents the coating time (in h).

2.3. Characterization of the modified membranes

To determine the thickness of the coating layer on membranes, PSf thin film was used as a model substrate. A 3 wt% PSf in cyclopentanone solution was spin-coated on a Si wafer using an MTC-100 vacuum spin coater (MicroNano Tools, Canada). The PSf films have thicknesses varying from 120 nm to 160 nm, with a variance less than 10% for each film. The PSf films were further coated with PDA+AZO using the technique described in Section 2.2. The thicknesses of the PSf and PDA+AZO layers were determined using an F20 Thin Film Analyzer (Filmetrics Inc., San Diego, CA). PSf has a refractive index value of 1.63 [47], and the PDA+AZO layer has a value of 1.62, an average of PDA (1.59) and AZO (1.65) [48]. Each thickness value reported in this study is an average of at least five locations on the film.

To determine the contact angles of the membrane surface, a Ramé-Hart goniometer (Model 190, Ramé-Hart Instrument Co., Succasunna, NJ) was used with a captive bubble method and a sessile drop method. For the captive bubble method, the membrane sample was attached to a sample holder and immersed in water in a transparent chamber to simulate membrane operation underwater. Droplets of \emph{n} -decane (2 μ L) were deposited on the membrane surface using a needle connected to a Gilmont microliter syringe (Cole-Parmer, Vernon Hills, IL). For the sessile drop method, DROPimage software (Ramé-Hart Instrument Co.) was utilized to obtain real-time values for the contact angles of water droplets (2 μ L) on the membrane surface. To analyze the effect of UV radiation on contact angle values, the membranes were exposed to UV LED penlight (wavelength or $\lambda = 365\,\text{nm}$) (Stylus*, Streamlight Inc., Eagleville, PA). In these measurements, a minimum of five droplets of liquid were analyzed, and the mean values are reported here.

Focused ion beam-scanning electron microscopy (FIB-SEM, Zeiss Auriga, Germany) was used to analyze the surface morphology of pristine and modified membranes. A sputtering coating apparatus was used to coat a thin layer of gold on the membrane samples. X-ray photoelectron spectrometer (XPS) (PHI 5600-CI, Physical Electronics, Chanhassen, MN) was used to analyze the elemental composition of the pristine and modified PSf dense films. Monochromatic Al K α X-rays with a pass energy of 58.7 eV was used. Percentages of elemental composition were calculated based on the relative areas of individual component peaks. The analysis was performed in two different regions for each sample.

2.4. Characterization of photoresponsive behavior

UV–Vis absorption spectroscopy was used to analyze the photoresponsive behavior of AZO. A solution containing AZO in DMF was tested using UV-3101PC spectrophotometer (Shimadzu Corp., Tokyo, Japan) with wavelengths (λ) ranging from 350 nm to 550 nm. For the PDA+AZO coating, the coated PSf thin films were mounted on a

transparent microscope cover glass (Erie Scientific, Portsmouth, NH). The samples were irradiated with the light of the desired wavelength using an RF-5301 PC spectrofluorophotometer (Shimadzu Corp.).

2.5. Determination of water permeance through the membranes

Pure water permeance was determined using a dead-end filtration system [49–51]. The membrane stamps with an active area of $11.5 \, \text{cm}^2$ were placed in permeation cells (UHP 43, Sterlitech Corp., Kent, WA), which were then filled with the DI water. Nitrogen was used to provide the feed pressure of 0.69 bar for PVDF and PSf membranes and 2.1 bar for PES membranes. The stirring rate was maintained at 350 rpm for PVDF and PSf membranes, and at 1000 rpm for PES membranes. Pure water permeance (A_W , L/m² h bar or LMH/bar) can be calculated using the following equation [52]:

$$A_W = \frac{1}{\Delta p. \, A_m. \, \rho_W} \frac{dm}{dt} \tag{1}$$

where Δp is the trans-membrane pressure (bar), A_m denotes the effective membrane area (cm²), ρ_W represents the density of water (g/cm³), and dm/dt refers to the rate of permeated water (g/h) [53]. For the modified membranes, the pure water permeance was determined approximately 48 h after modification.

BSA was selected as a model foulant to analyze the membrane performance and to demonstrate the self-cleaning behavior of the surface-modified membranes. 1 g/L BSA solution was prepared by dissolving lyophilized BSA powder in PBS solution at a pH value of 7.4. The water permeance of the modified membranes was measured using the dead-end filtration system, while the feed water was replenished to maintain the BSA concentration at 1 g/L.

To demonstrate the self-cleaning behavior of the PDA/AZO-coated membranes, the membrane samples were placed under a 30 W UV lamp ($\lambda=365$ nm) (UVP LLC, Upland, CA) for the desired time. In this study, one UV/vis cycle consists of exposing a membrane sample to UV light for 5 min and then visible light for 5 min. Two kinds of UV treatment were used, UV-3 and UV-6, where the number represents the number of UV/vis cycles. Water permeance was determined before and after the UV/vis cycles to elucidate the effect of self-cleaning on water permeance.

3. Results and discussion

3.1. Characterization of the PDA/AZO coating on model PSf dense films

To obtain accurate film thickness measurements, PSf dense films were used as the model substrate instead of UF membranes [6]. Fig. 3 shows the effect of AZO concentration in the coating solutions and coating time on the thickness of the coating layer. As shown in Fig. 3a, the coating with $2\,\mathrm{g/L}$ dopamine for $2\,\mathrm{h}$ yields a thickness of $16\,\mathrm{nm}$, which is similar to those reported in the literature [6,37,53]. Introduction of AZO in the coating solution increases the thickness of the coating layer. For instance, as the AZO concentration in the coating solution increases from zero to $2\,\mathrm{g/L}$ (2-PDA/2-AZO- $2\,\mathrm{h}$), the thickness of the coating layer increases from $16\,\mathrm{nm}$ to $37\,\mathrm{nm}$, which also suggests that the AZO content in the coating layer may increase to 57%.

Fig. 3b shows that increasing the coating time increases the layer thickness of 2-PDA/2-AZO. A control experiment was also performed by coating the PSf film with an only AZO solution. No increase in the film thickness was observed after the surface modification. Thus, these results confirm that PDA can graft AZO to form robust coating layers through the covalent and non-covalent bonding.

The coating layer on the surface of PSf thin films was characterized using XPS for elemental information [6,54]. Fig. 4 presents the N 1 s spectra of a virgin PSf film, a PDA coated, and a PDA/AZO coated PSf film. The PSf film does not have N peak, while the PDA coated one

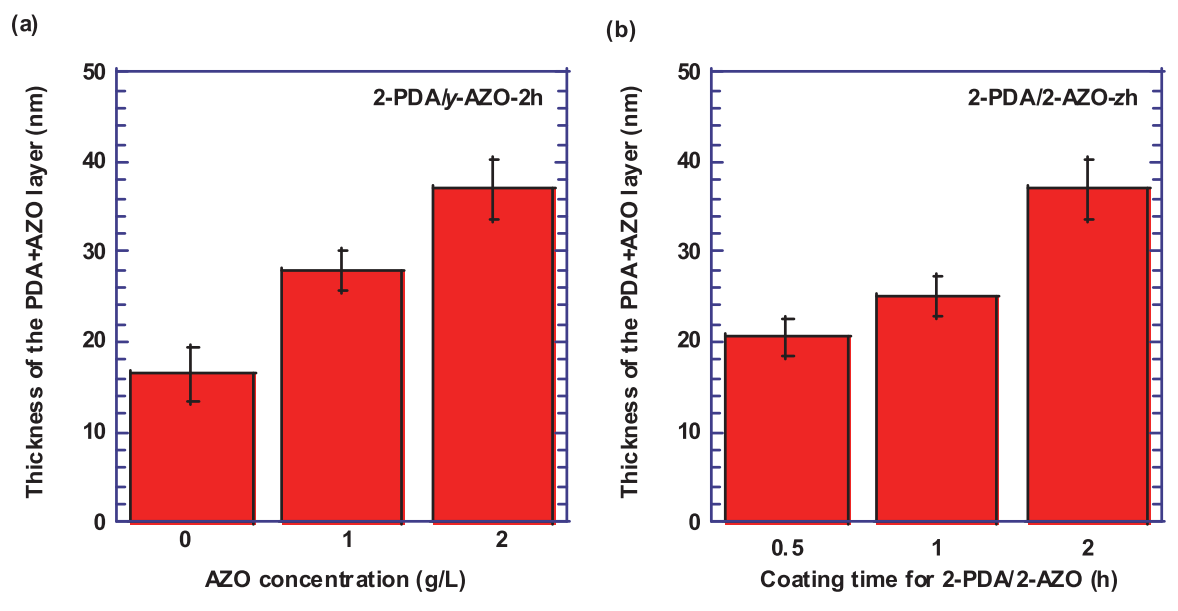


Fig. 3. The thickness of the coating layer (PDA or PDA/AZO) as a function of (a) AZO concentration in the coating solutions and (b) coating time.

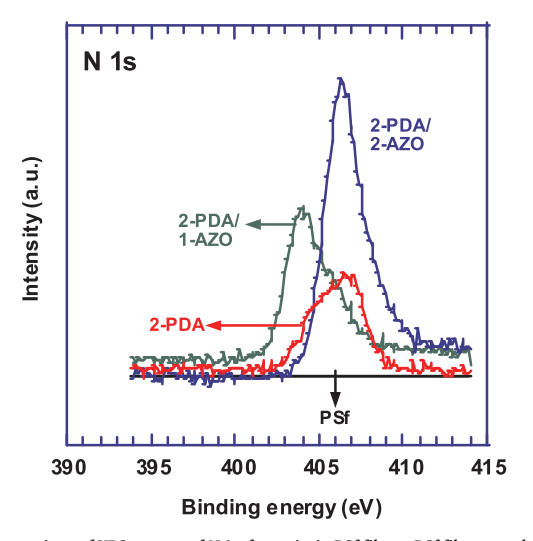


Fig. 4. Comparison of XPS spectra of N 1 s for a virgin PSf film, a PSf film coated with 2 g/L dopamine, and another two films coated with PDA/AZO for 2 h (i.e., 2-PDA/1-AZO and 2-PDA/2-AZO).

shows an N peak, indicating a successful coating of PDA. The introduction of AZO in the coating solution increases the N content in the coating layer, which is consistent with the theoretical analysis that AZO has 25% N and PDA has only 9% N. Increasing the AZO content in the coating solution also increases the N content in the coating layer. Additionally, the O content decreases from 27% for the PSf film to 24% for the PDA coated one. The introduction of 1 g/L AZO in the coating solution further decreases the O content to 18%. To put it into perspective, the theoretical O content in the PSf, PDA, and AZO is 12%, 18%, and 0%, respectively. The measured O content in PSf is higher than the theoretical value, presumably due to the formation of OH bonds on the surface of films. Both results of N and O confirm the successful coating of PDA and AZO on the PSf thin films.

3.2. Characterization of the PDA/AZO coating on membranes

Fig. 5a and b display the SEM images of a pristine PSf UF membrane and a PDA/AZO coated PSf membrane surface, respectively. The surface coating decreases the porosity of the membrane surface, while a substantial number of pores remain uncovered. This is consistent with

the hypothetical schematic of the surface modification shown in Fig. 2, and the results reported in the literature [6,37,53]. While the quantitative changes of pore size and porosity caused by the coating can be modelled using water permeance and MWCO measurement [53], it would be beyond the scope of this study to thoroughly investigate this effect. Fig. 5c shows the surface of a PDA/AZO-modified PSf membrane after being challenged with 1 g/L BSA solution. The presence of BSA on the membrane surface was observed. However, after exposing the fouled membrane surface to UV/vis cycles (UV-3), the BSA was removed, as shown in Fig. 5d, confirming the self-cleaning behavior of the PDA/AZO layer.

Fig. 6a presents the underwater contact angles of *n*-decane determined using the captive bubble method for the modified PSf and PVDF membranes. As expected, the PDA coating decreases the contact angles, indicating the enhanced surface hydrophilicity [6,36,37]. The addition of AZO in the coating solution further decreases the contact angle, presumably due to the hydrophilicity of the AZO with amine groups [55,56] and the change of surface morphology. However, due to the lack of the information about the detailed structure of PDA, it is impossible to directly compare the hydrophilicity between PDA and AZO. Nevertheless, the consistent trends in the PSf and PVDF membranes suggest the versatility of the approach to modifying membranes with different surface chemistries. The hydrophilicity enhancement seems to be less for PVDF than PSf because it is more challenging to coat the fluorinated PVDF than PSf.

Fig. 6b presents the effect of the coating time on the contact angle values for PSf membranes coated using PDA/AZO. Further increase in the coating time has a negligible effect on the contact angles, though the AZO content in the PDA/AZO layer increases with increasing coating time. Additionally, the AZO concentration in the coating solution has a negligible effect on the contact angles. For example, when AZO concentration increases from 1 to 2 g/L, the contact angle of the modified PSf membranes hardly changes from 39° to 38°.

The sessile drop method was also used to measure the contact angles of water to further illustrate the effect of surface modification on hydrophilicity. The pristine PSf membrane exhibits a contact angle of $78^{\circ} \pm 3^{\circ}$, whereas the PDA coated one has a contact angle of $52^{\circ} \pm 4^{\circ}$. For the PDA/AZO modified one, the contact angle is further reduced to $39^{\circ} \pm 2^{\circ}$.

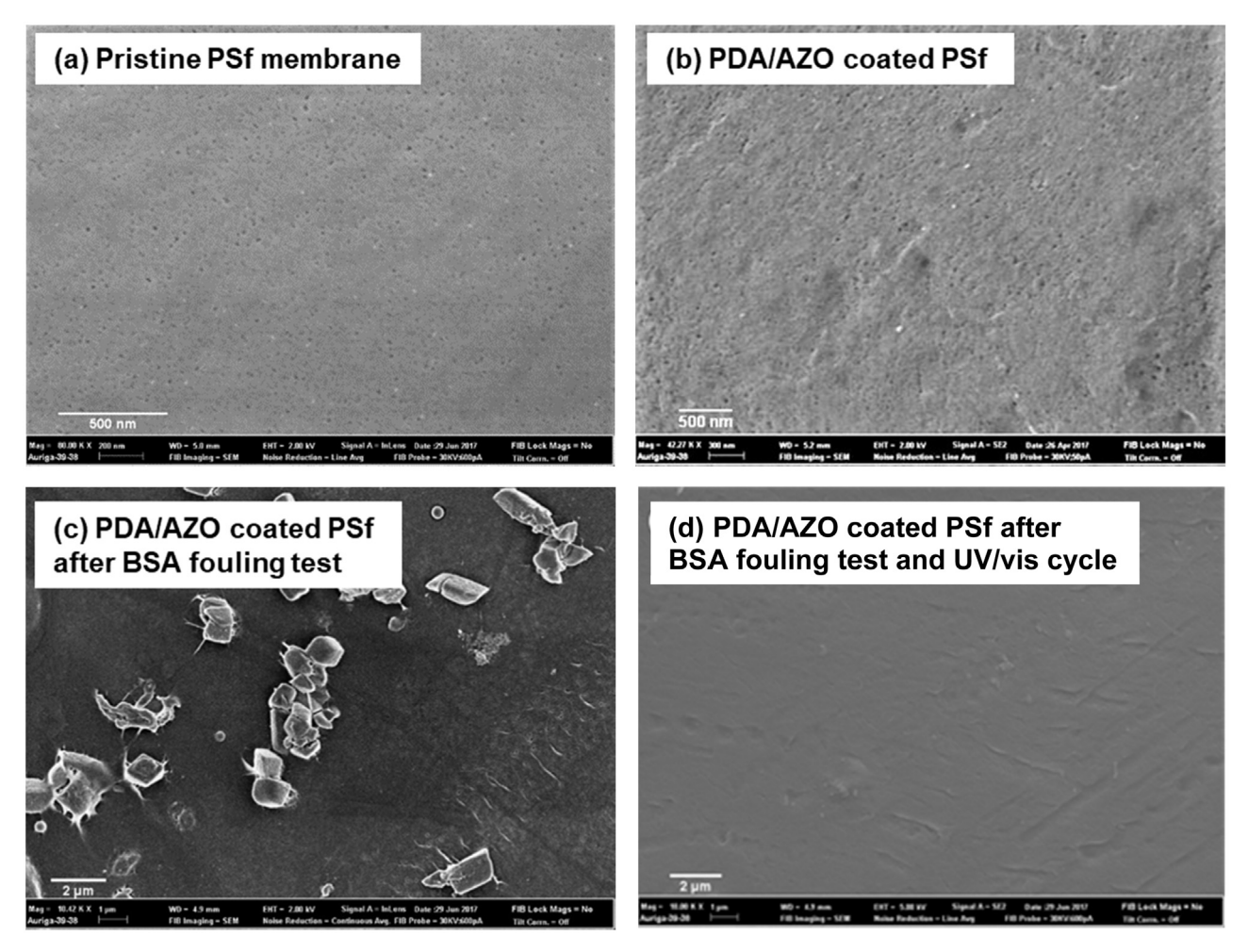


Fig. 5. SEM images of the surface for (a) a pristine PSf UF membrane, (b) PDA/AZO coated PSf membrane, (c) PDA/AZO coated PSf membrane after fouling test with 1 g/L BSA solution, and (d) PDA/AZO coated PSf membrane after being challenged with 1 g/L BSA solution followed by exposure to UV/vis cycles for self-cleaning.

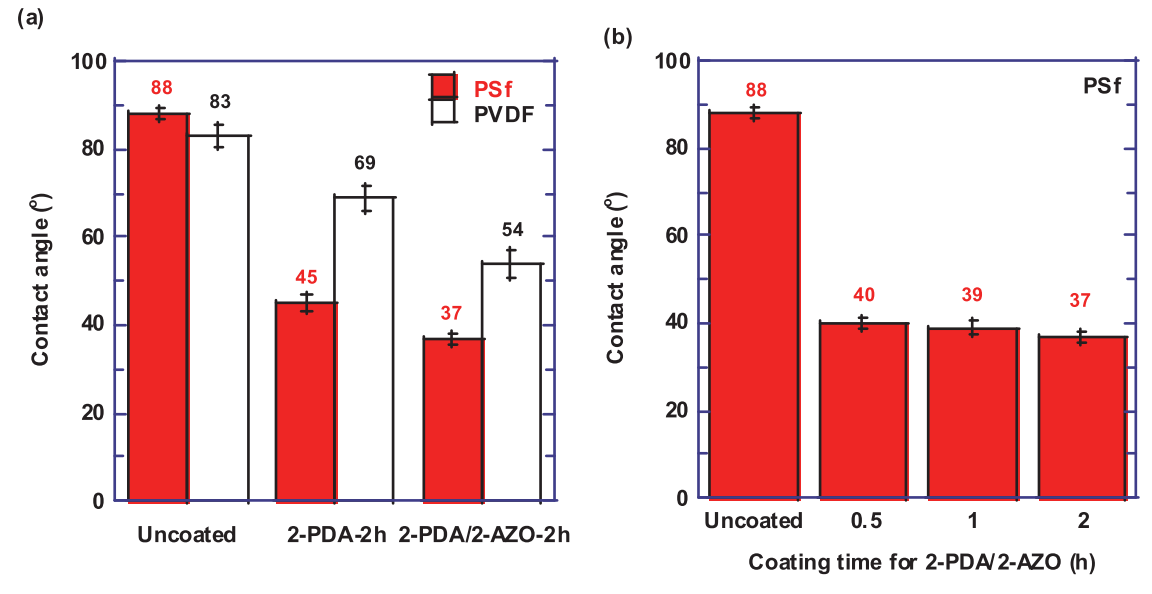


Fig. 6. (a) Effect of surface coating on the *n*-decane contact angles (determined using the captive bubble method) for PSf and PVDF membranes. (b) Effect of the coating time on the contact angles of the PSf membranes coated with 2-PDA/2-AZO.

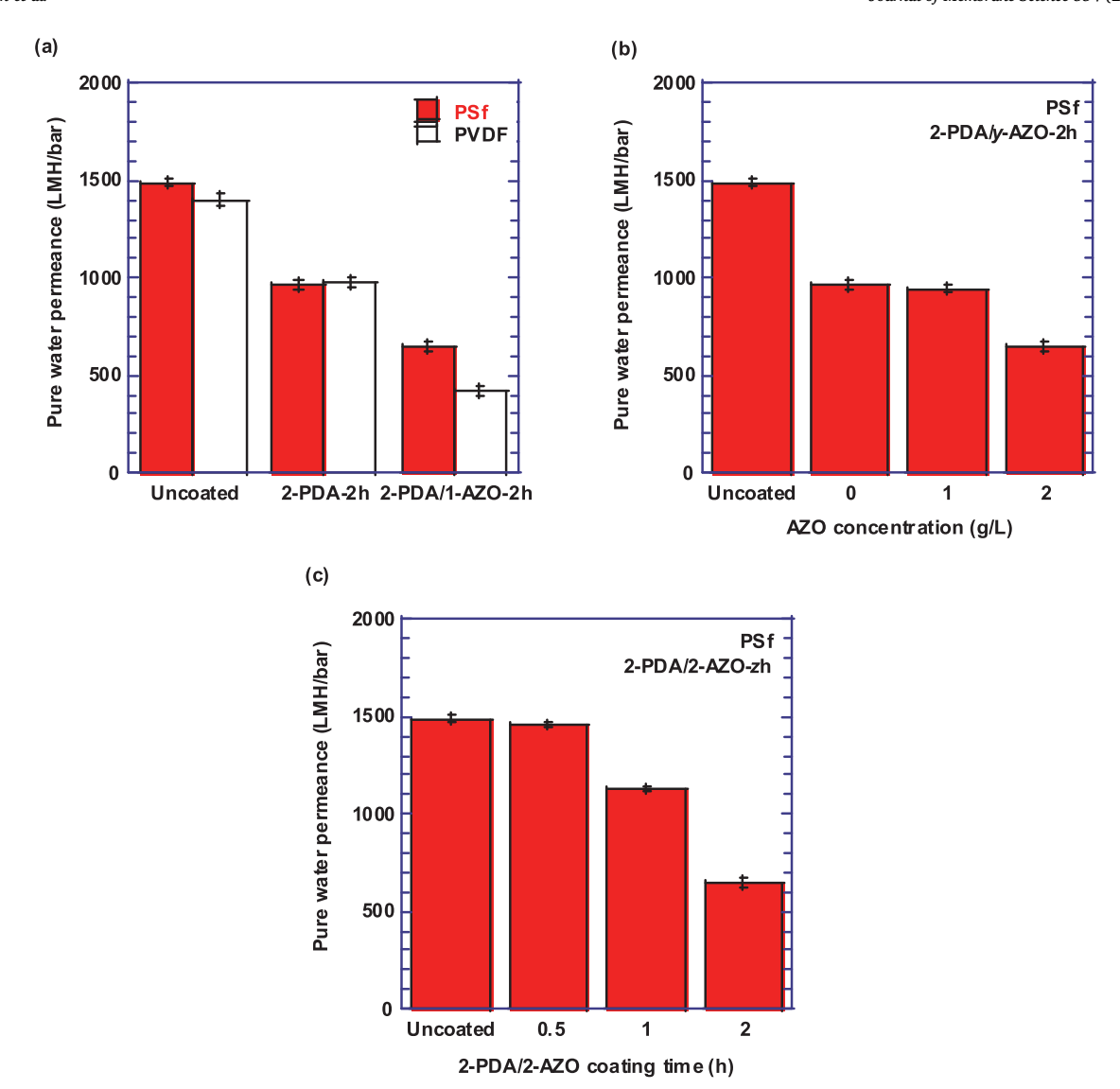


Fig. 7. (a) Effect of surface coating on pure water permeance for PSf and PVDF UF membranes, and the effect of (b) AZO concentration in the coating solutions and (c) the coating time on pure water permeance in PSf membranes.

3.3. Effect of the surface modification on pure water permeance

Fig. 7 displays the pure water permeance of the uncoated and modified PSf and PVDF UF membranes. The pure water permeance decreases with the surface coating. For instance, the PDA coating with an estimated thickness of 16 nm on PSf membranes decreases the water permeance from 1500 LMH/bar to 940 LMH/bar. In addition, the PDA/AZO with a thickness of 37 nm decreases the water permeance to 650 LMH/bar. Although the surface modification increases the hydrophilicity, the surface coating decreases the pore size and porosity and thus water permeance. Similar behavior has also been observed for PES UF membranes, where the PDA and PDA/AZO coating decreases the water permeance from 12 LMH/bar to 3.8 and 3.5 LMH/bar, respectively.

Fig. 7b shows the effect of AZO concentration in the coating solution on pure water permeance of PSf membranes. As the AZO concentration increases from 0 to 1 g/L in the coating solution, the water permeance remains unchanged, though the coating layer thickness increases from 16 nm to 25 nm. This behavior can be ascribed to the enhanced surface hydrophilicity when the AZO is introduced. In contrast, further increase of AZO concentration to 2 g/L decreases the pure water permeance due to the increased coating layer thickness and thus greater resistance. The contact angles barely change as the AZO concentration increases from 1

to 2 g/L, as discussed in Section 3.1.

Fig. 7c illustrates the effect of coating time on the pure water permeance in PSf membranes. Interestingly, the PDA/AZO coating for 0.5 h does not decrease the water permeance, compared with the uncoated membrane. This is likely due to the balanced effect of increased hydrophilicity and transport resistance derived from the coating. Further increase in the coating time reduces the water permeance caused by the dominant adverse effect of the increased resistance to water transport.

To test the stability of the PDA/AZO layer underwater, pure water permeance tests were repeated for the modified PVDF membranes, which were stored in DI water for approximately 9 months. The water permeance decreases by less than 5% for the aged sample, compared with the fresh sample, indicating the stability of the PDA + AZO layer on the membrane surface. This result is also consistent with the literature. For example, poly(ethylene glycol) amine (PEG-NH₂) was graft on the membrane surface through PDA, and the membrane was demonstrated to be stable in a field test for treating flowback water from hydraulic shale fracturing [57].

The ideal membranes should have high water permeance, low water contact angle, and thick PDA+AZO layer to exhibit self-cleaning behavior. In this study, PSf membrane coated with 2-PDA/1-AZO-2 h were selected for further evaluation. This modified membrane has balanced

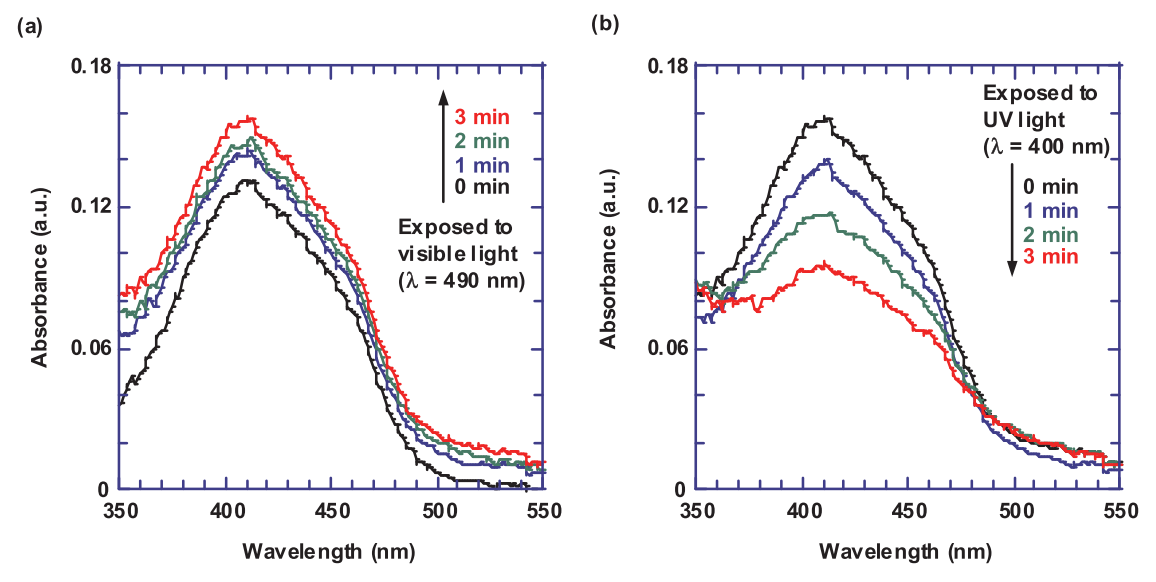


Fig. 8. Photoisomerization of 1 mg/L AZO in DMF upon exposure to the (a) visible light ($\lambda = 490 \, \text{nm}$) and (b) UV light ($\lambda = 400 \, \text{nm}$) as a function of exposure time.

properties, including a pure water permeance of about 940 LMH/bar, a contact angle of 37°, and a PDA/AZO layer thickness of 25 nm.

3.4. Photoresponsive behavior

3.4.1. Photoresponsive behavior of AZO in solutions

Fig. 8 displays the UV-Vis absorption spectra of 1 mg/L AZO in DMF upon exposure to UV and visible light. AZO displays a significant π - $\pi\,^*$ transition band at 408 nm and a weak sub-band at 461 nm corresponding to the overlap between the $n-\pi$ * and the vibronic transition bands [58,59]. AZO was exposed to the light of 400 nm and 490 nm wavelengths to induce the π - π * transition and thus the isomerization [60-63]. In the absence of UV light, AZO exists predominantly in the trans form. As shown in Fig. 8a, when AZO is irradiated with the visible light ($\lambda = 490 \text{ nm}$), the absorbance at 408 nm increases, confirming the increased proportion of trans-AZO [42,61-64]. After 3 min exposure to the visible light, the magnitude of absorbance at 408 nm does not increase further, indicating that the AZO attains trans-dominant photostationary state. In contrast, when the AZO is irradiated with the UV light ($\lambda = 400 \text{ nm}$), the absorbance at 408 nm decreases (Fig. 8b), indicating the trans to cis transition [42,61-64]. The isomerization reaches cis-AZO-dominant photostationary state after 3 min exposure to the UV light since the magnitude of absorbance at 408 nm levels off.

To illustrate the reversible switching behavior, the AZO solution was irradiated with visible light for 3 min, and then with UV light for 3 min. This cycle was repeated for three times, and the resulting variation in the absorbance at 408 nm as a function of time is depicted in Fig. 9a. The absorbance consistently increases with the exposure to visible light and then decreases with the exposure to UV light. The pattern indicates the reversibility of the isomerization of the AZO, which had also been reported for other azobenzene-based derivatives [65–68].

3.4.2. Photoresponsive behavior of a coating layer of PDA/AZO

Fig. 9b demonstrates the photoresponsive behavior for a PSf thin film coated with 2-PDA/1-AZO-2 h. The 2-PDA/1-AZO layer has a thickness of 25 nm. The absorbance peak corresponding to π - π * transition is observed at $\lambda=400$ nm, which is slightly lower than that for the AZO in DMF solution. This behavior could be due to the interactions (such as the π - π stacking or hydrogen bonding) between the PDA and AZO. Additionally, the PSf/PDA-AZO film attains photochemical equilibrium after 5-min irradiation with visible or UV light. As shown in Fig. 9b, the PSf/PDA-AZO film displays a reversible switching behavior

similar to that of AZO solution. The existence of the repeatable pattern also signifies successful deposition of AZO on the PSf surface.

Another way to confirm the photoresponsive behavior is the contact angles determined using the sessile drop method. The cis-AZO has greater polarity than the trans-AZO and thus greater hydrophilicity. Fig. 10a displays the contact angle values as a function of UV exposure time for membranes coated with different AZO concentrations. As expected, the PDA coated PSf membrane does not show changes in the contact angles due to the absence of photoresponsive property. However, for the PDA/AZO coated membranes, the UV exposure decreases the contact angles. For example, for the 2-PDA/2-AZO coated membrane, the UV exposure decreases the contact angle from 39° to 29°. On the other hand, increase in the UV exposure time has minimal effect on the contact angles. The decreased water contact angle indicates the enhanced surface hydrophilicity as expected for the trans to cis transition. Similar changes in the contact angles of azobenzene-containing surfaces in the presence of UV light have also been noted in the literature [42,43,65,69-72].

Fig. 10b presents the effect of UV exposure on the water contact angles of 2-PDA/2-AZO coated PSf membranes for different coating times. All modified membranes show a similar trend, i.e., UV exposure decreases the water contact angle, which is again consistent with the expected transition of *trans*-AZO to more hydrophilic *cis*-AZO.

3.5. Self-cleaning of the photo-mobile membrane surface

The self-cleaning behavior of the modified membranes was demonstrated by the repeated testing with pure water and 1 g/L BSA solution. Fig. 11 depicts the relative water permeance (defined as the ratio of the water permeance at any time to the initial pure water permeance) as a function of operating time for the surface modified PSf membranes. The membranes were tested in a dead-end filtration system in the following order, pure water (labeled as W₀), BSA solution (BSA₁), pure water (W₁), UV/vis treatment, pure water (W₂), and BSA solution (BSA2). Fig. 11a shows the behavior of a PSf membrane coated with 2 g/L PDA as a baseline. Water permeance decreased when the membrane was challenged with the BSA solution due to the BSA fouling. The re-test with pure water recovers water permeance (as shown as W₁). The UV/vis cycle has not resulted in any appreciable improvement in membrane performance due to the absence of photo-mobile AZO. A slight increase in the pure water permeance for the membrane without UV treatment caused by the removal of BSA on the membrane surface when rinsing.

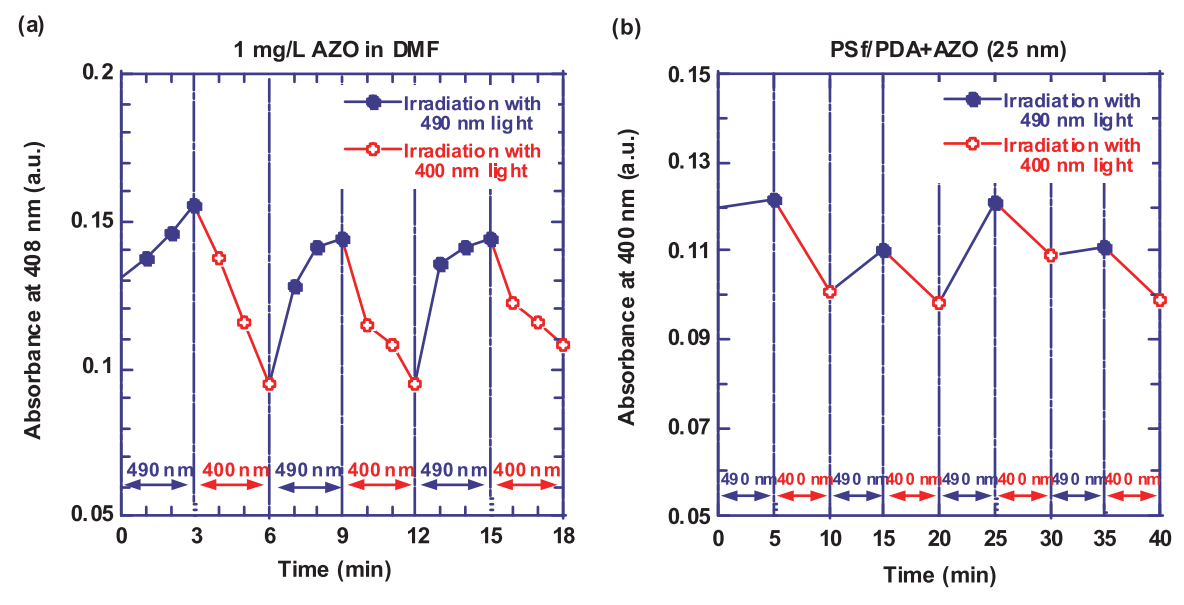


Fig. 9. Reversible isomerization of AZO when exposed alternatively to visible light ($\lambda = 490 \, \text{nm}$) and UV light ($\lambda = 400 \, \text{nm}$) for (a) 1 mg/L AZO in DMF and (b) PSf thin films with a 25-nm layer of 2-PDA/1-AZO coating.

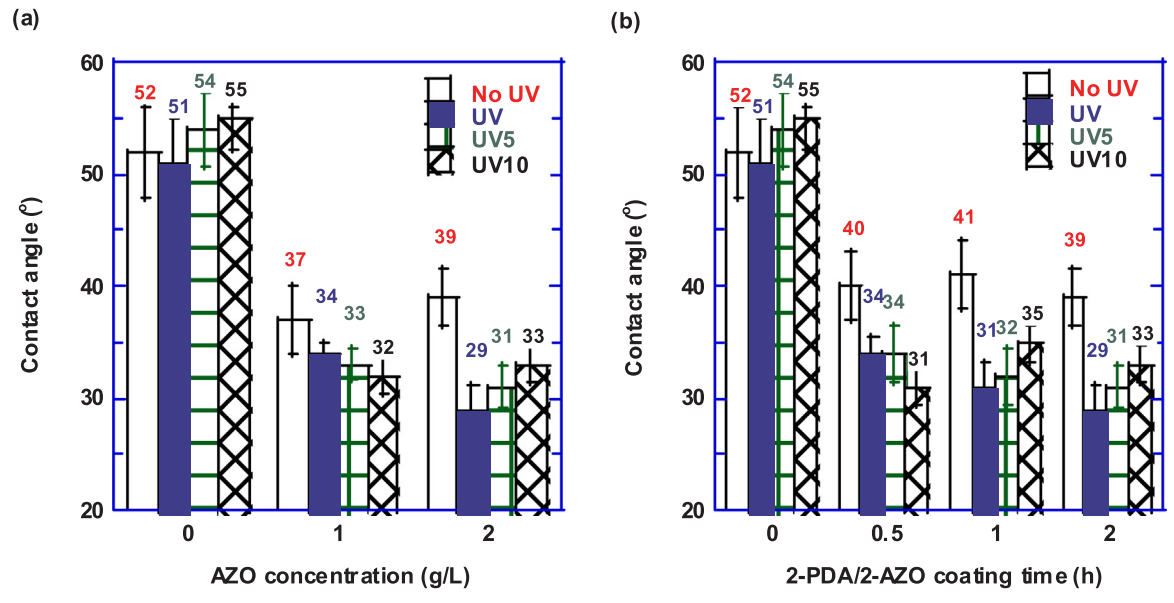


Fig. 10. Water contact angles as a function of (a) AZO concentration in the coating solution (2-PDA/y-AZO-2h) and (b) coating time for PSf UF membranes (2-PDA/2-AZO-zh). The nomenclature of UV, UV5, and UV10 indicates the time for the contact angle measurement after UV exposure, which is very short time, 5 min and 10 min, respectively.

Fig. 11b displays the membrane performance and the self-cleaning ability of 2-PDA/1-AZO-2h coated PSf membrane. As expected, exposure to BSA solution decreases water permeance, and the re-test with pure water recovers the water permeance. The UV/vis exposure (3 or 6 cycles) significantly increases the pure water permeance (W2), and the permeance during BSA fouling test (BSA2). However, if the membrane is not exposed to the UV/vis cycle, there is no change in pure water permeance (W2), and another test with the BSA solution further decreases water permeance. For instance, during the BSA2 test, the UV/vis treated membrane (UV-3) has a relative water permeance of about 0.34 (i.e., 440 LMH/bar), while the membrane without exposure to UV/vis cycles has a relative water permeance of about 0.12 (i.e., 170 LMH/ bar). In other words, the self-cleaned membranes show ~160% increase in the water permeance. Additionally, there is no significant difference in membrane performance between 3 and 6 cycles of UV/vis exposure. The effect of "self-cleaning" on the fouling is also imaged using SEM and shown in Fig. 5c and d. The absence of BSA on the surface of the

cleaned membrane demonstrates the advantage of PDA/AZO coating.

Similar experiments were performed on the PES UF membranes to further demonstrate the self-cleaning behavior in the PDA/AZO layer. As shown in Fig. 12a, the UV/vis treatment has a negligible effect on the PES membrane coated with only PDA. When the membrane is coated with PDA/AZO, the pure-water permeance (W₂) recovers after the UV/vis cycles. In addition, the water permeance with BSA solution (BSA₂) for UV/vis treated membrane is much higher than that of the membrane without the UV/vis treatment (Fig. 12b). Both Figs. 11b and 12b demonstrate the successful incorporation of AZO on the membrane surface through the bio-glue PDA and the consequent promising self-cleaning properties of the employed technique.

4. Conclusion

This work demonstrates that photo-mobile 4,4'-azodianiline can be co-deposited with bio-adhesive PDA onto UF membrane surface, which

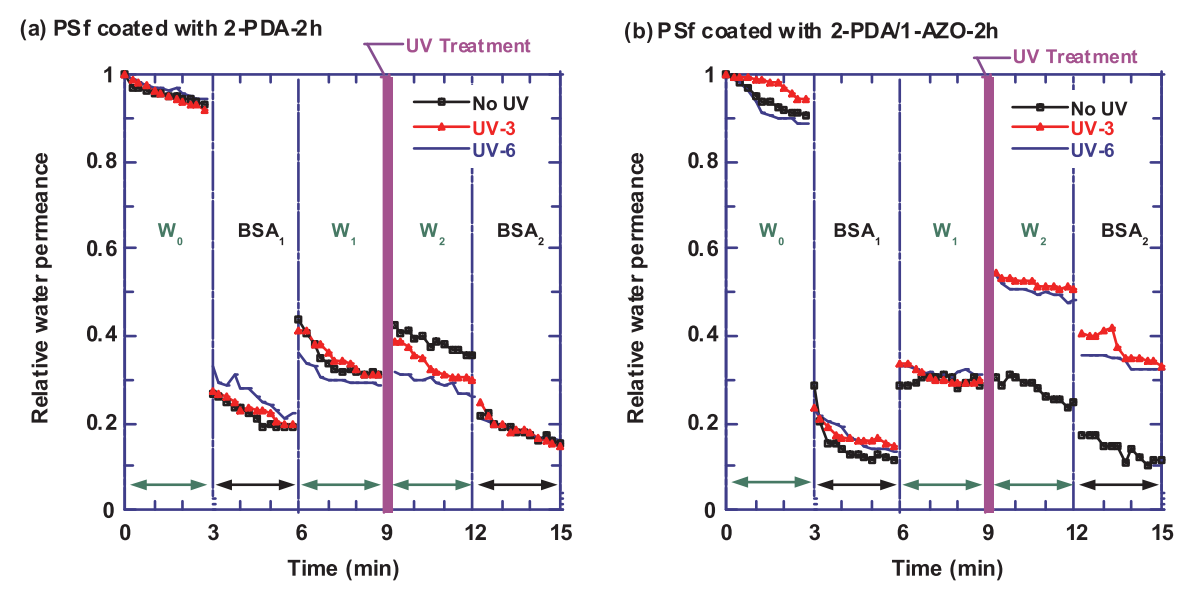


Fig. 11. Demonstration of the self-cleaning behavior by comparing the relative water permeance for (a) the 2-PDA-2 h modified PSf membranes with (b) the 2-PDA/1-AZO-2 h coated PSf membranes. The membranes were challenged with pure water (W₀), 1 g/L BSA solution (BSA₁), pure water (W₁), UV/vis exposure, pure water (W₂), and BSA solution (BSA₂).

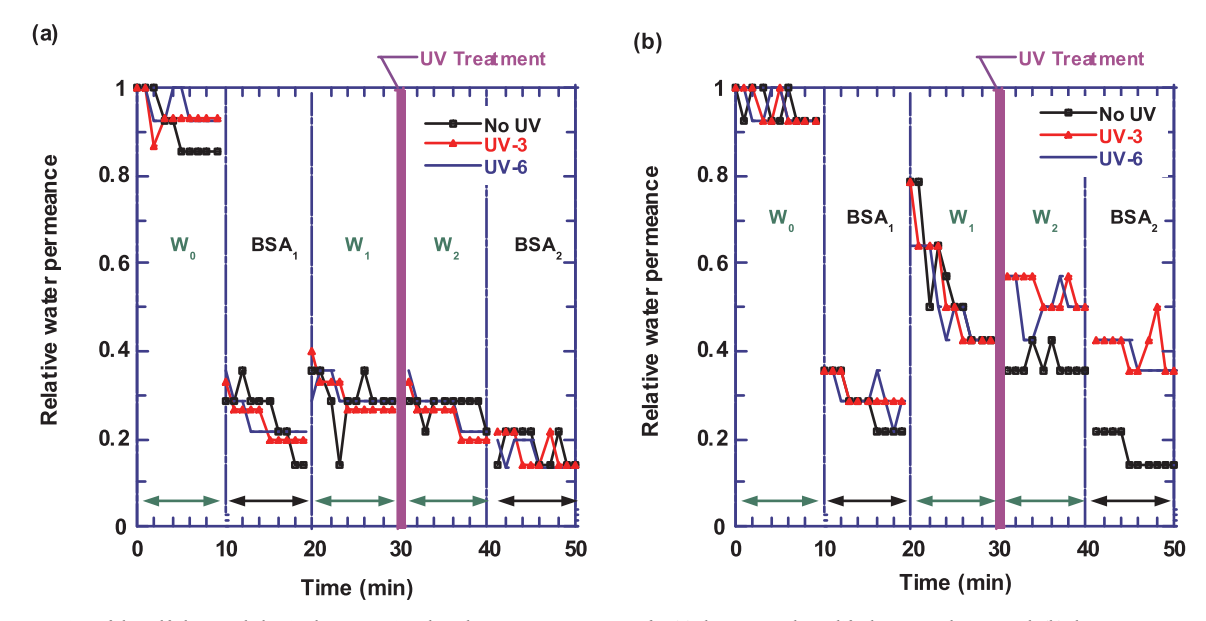


Fig. 12. Demonstration of the self-cleaning behavior by comparing the relative water permeance for (a) the 2-PDA-2 h modified PES membranes with (b) the 2-PDA/1-AZO-2 h modified PES membranes.

exhibits self-cleaning behavior and mitigates membrane fouling when exposed to UV and visible light alternatively. The co-deposition of PDA and AZO leads to a $10-50\,\mathrm{nm}$ thin layer on the solid portion of the membrane surface without covering the pores. The thickness of the coating layer increases with increasing coating time and AZO concentration in the coating solutions. The coating was verified using XPS and SEM. Although the coating layer of PDA/AZO enhances surface hydrophilicity, it decreases water permeance caused by the additional resistance to water transport.

The reversible photoresponsive behavior of AZO in solution and thin films with PDA was validated using UV–Vis absorption spectroscopy. Upon exposure to UV light, the water contact angle of a PDA/AZO coated PSf membrane decreases by 10°. During the fouling test, the PDA/AZO modified membranes with UV treatment increased water permeance by almost 160% compared with those without the UV exposure. This validates the effectiveness of this photo-mobile material for self-cleaning membrane surface. Because this facile one-step modification of membrane surface occurs in aqueous solution, it can be

readily applied as post-modification for membranes and modules.

Acknowledgements

We gratefully acknowledge the financial support of this work by the U.S. National Science Foundation Division of Civil, Mechanical and Manufacturing Innovation (CMMI) with a grant number of 1635026. We also thank the partial support from the SMART Communities of Excellence at University at Buffalo.

References

- M.A. Shannon, P.W. Bohn, M. Elimelech, J.G. Georgiadis, B.J. Mariñas, A.M. Mayes, Science and technology for water purification in the coming decades, Nature 452 (2008) 301–310.
- [2] G.M. Geise, H.S. Lee, D.J. Miller, B.D. Freeman, J.E. Mcgrath, D.R. Paul, Water purification by membranes: the role of polymer science, J. Polym. Sci. Part B. Polym. Phys. 48 (2010) 1685–1718.
- [3] H. Park, J. Kamcev, L.M. Robeson, M. Elimelech, B.D. Freeman, Maximizing the

- right stuff: the trade-off between membrane permeability and selectivity, Science 356 (2017) eaab0530.
- [4] D. Rana, T. Matsuura, Surface modifications for antifouling membranes, Chem. Rev. 110 (2010) 2448–2471.
- [5] D. Miller, D. Dreyer, C. Bielawski, D. Paul, B. Freeman, Surface modification of water purification membranes: a review, Angew. Chem. Int. Ed. 56 (2017) 4662–4711.
- [6] N. Shahkaramipour, S.N. Ramanan, D. Fister, E. Park, S.R. Venna, H.T. Sun, C. Cheng, H. Lin, Facile grafting of zwitterions onto the membrane surface to enhance antifouling properties for wastewater reuse, Ind. Eng. Chem. Res. 56 (2017) 9202–9212
- [7] R. Zhang, Y. Liu, M. He, Y. Su, X. Zhao, M. Elimelech, Z. Jiang, Antifouling membranes for sustainable water purification: strategies and mechanisms, Chem. Soc. Rev. 45 (2016) 5888–5924.
- [8] N. Shahkaramipour, T. Tran, S. Ramanan, H. Lin, Membranes with surface-enhanced antifouling properties for water purification, Membranes 7 (2017) 13.
- [9] X. Shi, G. Tal, N.P. Hankins, V. Gitis, Fouling and cleaning of ultrafiltration membranes: a review, J. Water Process Eng. 1 (2014) 121–138.
- [10] Ś.F.E. Boerlage, M.D. Kennedy, M.P. Aniye, E.M. Abogrean, D.E.Y. El-Hodali, Z.S. Tarawneh, J.C. Schippers, Modified fouling index_(ultrafiltration) to compare pretreatment processes of reverse osmosis feedwater, Desalination 131 (2000) 201–214
- [11] Y. Ding, S. Maruf, M. Aghajani, A.R. Greenberg, Surface patterning of polymeric membranes and its effect on antifouling characteristics, Sep. Sci. Technol. 52 (2017) 240–257
- [12] S.H. Maruf, M. Rickman, L. Wang, J. Mersch, A.R. Greenberg, J. Pellegrino, Y. Ding, Influence of sub-micron surface patterns on the deposition of model proteins during active filtration, J. Membr. Sci. 444 (2013) 420–428.
- [13] S.H. Maruf, L. Wang, A.R. Greenberg, J. Pellegrino, Y. Ding, Use of nanoimprinted surface patterns to mitigate colloidal deposition on ultrafiltration membranes, J. Membr. Sci. 428 (2013) 598–607.
- [14] S.T. Weinman, S.M. Husson, Influence of chemical coating combined with nanopatterning on alginate fouling during nanofiltration, J. Membr. Sci. 513 (2016) 146–154.
- [15] O. Velicangil, J.A. Howell, Self-cleaning membranes for ultrafiltration, Biotechnol. Bioeng. 23 (1981) 843–854.
- [16] S. Darvishmanesh, X. Qian, S.R. Wickramasinghe, Responsive membranes for advanced separations, Curr. Opin. Chem. Eng. 8 (2015) 98–104.
- [17] Z. Liu, W. Wang, R. Xie, X. Ju, L. Chu, Stimuli-responsive smart gating membranes, Chem. Soc. Rev. 45 (2016) 460–474.
- [18] D. Wandera, S.R. Wickramasinghe, S.M. Husson, Stimuli-responsive membranes, J. Membr. Sci. 357 (2010) 6–35.
- [19] J.I. Clodt, V. Filiz, S. Rangou, K. Buhr, C. Abetz, D. Hoche, J. Hahn, A. Jung, V. Abetz, Double stimuli-responsive isoporous membranes via post-modification of pH-sensitive self-assembled diblock copolymer membranes, Adv. Funct. Mater. 23 (2013) 731–738.
- [20] H.H. Himstedt, K.M. Marshall, S.R. Wickramasinghe, pH-responsive nanofiltration membranes by surface modification, J. Membr. Sci. 366 (2011) 373–381.
- [21] M. Dubner, M.E. Naoum, N.D. Spencer, C. Padeste, From pH-to light-response: postpolymerization modification of polymer brushes grafted onto microporous polymeric membranes, ACS Omega 2 (2017) 455–461.
- [22] M. Birkner, M. Ulbricht, Ultrafiltration membranes with markedly different pH- and ion-responsivity by photografted zwitterionic polysulfobetain or polycarbobetain, J. Membr. Sci. 494 (2015) 57–67.
- [23] G. Song, S.R. Wickramasinghe, X. Qian, The effects of salt type and salt concentration on the performance of magnetically activated nanofiltration membranes, Ind. Eng. Chem. Res. 56 (2017) 1848–1859.
- [24] S. Frost, M. Ulbricht, Thermoresponsive ultrafiltration membranes for the switchable permeation and fractionation of nanoparticles, J. Membr. Sci. 448 (2013) 1–11
- [25] F.P. Nicoletta, D. Cupelli, P. Formoso, G. De Filpo, V. Colella, A. Gugliuzza, Light responsive polymer membranes: a review, Membranes 2 (2012) 134–197.
- [26] A. Nayak, H.W. Liu, G. Belfort, An optically reversible switching membrane surface, Angew. Chem. Int. Ed. 45 (2006) 4094–4098.
- [27] P. Kaner, X.R. Hu, S.W. Thomas, A. Asatekin, Self-cleaning membranes from combshaped copolymers with photoresponsive side groups, ACS Appl. Mater. Inter. 9 (2017) 13619–13631.
- [28] F. Ercole, T.P. Davis, R.A. Evans, Photo-responsive systems and biomaterials: photochromic polymers, light-triggered self-assembly, surface modification, fluorescence modulation and beyond, Polym. Chem. 1 (2010) 37–54.
- [29] A.C. Pauly, K. Schöller, L. Baumann, R.M. Rossi, K. Dustmann, U. Ziener, D. de Courten, M. Wolf, L.F. Boesel, L.J. Scherer, ATRP-based synthesis and characterization of light-responsive coatings for transdermal delivery systems, Sci. Tech. Adv. Mater. 16 (2015) 034604.
- [30] H. Rau, Spectroscopic properties of organic azo compounds, Angew. Chem. Int. Ed. 12 (1973) 224–235.
- [31] G.S. Hartley, R.J.W. Le Fevre, The dipole moments of cis- and trans-azobenzenes and of some related compounds, J. Chem. Soc. (1939) 531–535.
- [32] M. Kondo, R. Miyasato, Y. Naka, J.-I. Mamiya, M. Kinoshita, Y. Yu, C.J. Barrett, T. Ikeda, Photomechanical properties of azobenzene liquid-crystalline elastomers, Liq. Cryst. 36 (2009) 1289–1293.
- [33] T. Kinoshita, M. Sato, A. Takizawa, Y. Tsujita, Photocontrol of polypeptide membrane functions by cis-trans isomerization in side-chain azobenzene groups, Macromolecules 19 (1986) 51–55.
- [34] K. Weh, M. Noack, R. Ruhmann, K. Hoffmann, P. Toussaint, J. Caro, Modification of the transport properties of a polymethacrylate-azobenzene membrane by

- photochemical switching, Chem. Eng. Technol. 21 (1998) 408-412.
- [35] B. Tylkowski, S. Peris, M. Giamberini, R. Garcia-Valls, J.A. Reina, J.C. Ronda, Light-induced switching of the wettability of novel asymmetrical poly(vinyl alcohol)-coethylene membranes blended with azobenzene polymers, Langmuir 26 (2010) 14821–14829.
- [36] B.D. McCloskey, H. Park, H. Ju, B.W. Rowe, D.J. Miller, B.J. Chun, K. Kin, B.D. Freeman, Influence of polydopamine deposition conditions on pure water flux and foulant adhesion resistance of reverse osmosis, ultrafiltration, and microfiltration membranes, Polymer 51 (2010) 3472–3485.
- [37] B.D. McCloskey, H. Park, H. Ju, B.W. Rowe, D.J. Miller, B.D. Freeman, A bioinspired fouling-resistant surface modification for water purification membranes, J. Membr. Sci. 413–414 (2012) 82–90.
- [38] D.R. Dreyer, D.J. Miller, B.D. Freeman, D.R. Paul, C.W. Bielawski, Perspectives on poly(dopamine), Chem. Sci. 4 (2013) 3796–3802.
- [39] H. Chen, W.-S. Hung, C.-H. Lo, S.-H. Huang, M.-L. Cheng, G. Liu, K.-R. Lee, J.-Y. Lai, Y.-M. Sun, C.-C. Hu, Free-volume depth profile of polymeric membranes studied by positron annihilation spectroscopy: layer structure from interfacial polymerization, Macromolecules 40 (2007) 7542–7557.
- [40] R. Zhou, P. Ren, H. Yang, Z. Xu, Fabrication of antifouling membrane surface by poly(sulfobetaine methacrylate)/polydopamine co-deposition, J. Membr. Sci. 466 (2014) 18–25.
- [41] H. Lee, S.M. Dellatore, W.M. Miller, P.B. Messersmith, Mussel-inspired surface chemistry for multifunctional coatings, Science 318 (2007) 426–430.
- [42] C. Kallweit, M. Bremer, D. Smazna, T. Karrock, R. Adelung, M. Gerken, Photoresponsive hierarchical ZnO-PDMS surfaces with azobenzene-polydopamine coated nanoparticles for reversible wettability tuning, Vacuum 146 (2017) 386–395
- [43] J. Zhang, W. Zhang, N. Zhou, Y. Weng, Z. Hu, Photoresponsive superhydrophobic surfaces from one-pot solution spin coating mediated by polydopamine, RSC Adv. 4 (2014) 24973–24977.
- [44] D.J. Miller, D.R. Paul, B.D. Freeman, An improved method for surface modification of porous water purification membranes, Polymer 55 (2014) 1375–1383.
- [45] Y. Baek, B.D. Freeman, A.L. Zydney, J. Yoon, A facile surface modification for antifouling reverse osmosis membranes using polydopamine under UV irradiation, Ind. Eng. Chem. Res. 56 (2017) 5756–5760.
- [46] K. Feng, L. Hou, B. Tang, P. Wu, A self-protected self-cleaning ultrafiltration membrane by using polydopamine as a free-radical scavenger, J. Membr. Sci. 490 (2015) 120–128.
- [47] S.L. Lane, R.L. Lindstrom, J.D. Cameron, R.H. Thomas, E.A. Mindrup, G.O. Waring, B.E. McCarey, P.S. Binder, Polysulfone corneal lenses, J. Cataract Refract. Surg. 12 (1986) 50–60.
- [48] B. Zhu, S. Edmondson, Polydopamine-melanin initiators for surface-initiated ATRP, Polymer 52 (2011) 2141–2149.
- [49] H. Ju, A.C. Sagle, B.D. Freeman, J.I. Mardel, A.J. Hill, Characterization of sodium chloride and water transport in crosslinked poly(ethylene oxide) hydrogels, J. Membr. Sci. 358 (2010) 131–141.
- [50] S. Shah, J. Liu, S. Ng, S. Luo, R. Guo, C. Cheng, H. Lin, Transport properties of small molecules in zwitterionic polymers, J. Polym. Sci. Part B. Polym. Phys. 54 (2016) 1924–1934.
- [51] T.N. Tran, S.N. Ramanan, H. Lin, Synthesis of hydrogels with antifouling properties as membranes for water purification, J. Vis. Exp. (2017) e55426.
- [52] S. Zhao, K. Huang, H. Lin, Impregnated membranes for water purification using forward osmosis, Ind. Eng. Chem. Res. 54 (2015) 12354–12366.
- [53] S. Kasemset, L. Wang, Z. He, D.J. Miller, A. Kirschner, B.D. Freeman, M.M. Sharma, Influence of polydopamine deposition conditions on hydraulic permeability, sieving coefficients, pore size and pore size distribution for a polysulfone ultrafiltration membrane, J. Membr. Sci. 522 (2017) 100–115.
- [54] C.-C. Chang, K.W. Kolewe, Y. Li, I. Kosif, B.D. Freeman, K.R. Carter, J.D. Schiffman, T. Emrick, Underwater superoleophobic surfaces prepared from polymer zwitterion/dopamine composite coatings, Adv. Mater. Interfaces 3 (2016) 1500521.
- [55] X. Pei, A. Fernandes, B. Mathy, X. Laloyaux, B. Nysten, O. Riant, A. Jonas, Correlation between the structure and wettability of photoswitchable hydrophilic azobenzene monolayers on silicon, Langmuir 27 (2011) 9403–9412.
- [56] X. Jiang, X. Zhang, J. Yuan, G. Cheng, Y. Li, Y. Huang, Z. Du, Aggregation and self-organization of hydrophilic azobenzene dye langmuir-blodgett films, Thin Solid Films 496 (2006) 595–600.
- [57] D.J. Miller, X. Huang, H. Li, S. Kasemset, A. Lee, D. Agnihotri, T. Hayes, D.R. Paul, B.D. Freeman, Fouling-resistant membranes for the treatment of flowback water from hydraulic shale fracturing: a pilot study, J. Membr. Sci. 437 (2013) 265–275.
- [58] H. Mustroph, Studies on the UV–Vis absorption spectra of azo dyes: part 25. analysis of the fine structure of the π₁ →π₁* band of 4′-donor-substituted 4-N,N-diethylaminoazobenzenes, Dyes Pigm. 15 (1991) 129–137.
- [59] H. Mustroph, Studies on UV/vis absorption spectra of azo dyes. part 26. electronic absorption spectra of 4,4'-diaminoazobenzenes, Dyes Pigm. 16 (1991) 223–230.
- [60] H.-C. Kang, B.M. Lee, J. Yoon, M. Yoon, Synthesis and surface-active properties of new photosensitive surfactants containing the azobenzene group, J. Colloid Interface Sci. 231 (2000) 255–264.
- [61] B. Yu, X. Jiang, R. Wang, J. Yin, Multistimuli responsive polymer nanoparticles on the basis of the amphiphilic azobenzene-contained hyperbranched poly(ether amine) (hPEA-AZO), Macromolecules 43 (2010) 10457–10465.
- [62] N.R. Krekiehn, M. Müller, U. Jung, S. Ulrich, R. Herges, O.M. Magnussen, UV/Vis spectroscopy studies of the photoisomerization kinetics in self-assembled azobenzene-containing adlayers, Langmuir 31 (2015) 8362–8370.
- [63] S. Chen, W. Wang, W. Xu, A photoresponsive azobenzene-graphene-gold nanocomposite using cationic azobenzene-surfactant as stabilizers and its electrochemical behavior. Mater. Lett. 180 (2016) 196–199.

- [64] S.K. Kumar, J.-D. Hong, C.-K. Lim, S.-Y. Park, Synthesis and photoisomerization characteristics of a 2,4,4'-substituted azobenzene tethered to the side chains of polymethacrylamide, Macromolecules 39 (2006) 3217–3223.
- [65] P. Dietrich, F. Michalik, R. Schmidt, C. Gahl, G. Mao, M. Breusing, M.B. Raschke, B. Priewisch, T. Elsässer, R. Mendelsohn, M. Weinelt, K. Rück-Braun, An anchoring strategy for photoswitchable biosensor technology: azobenzene-modified SAMs on Si(111), Appl. Phys. A. 93 (2008) 285–292.
- [66] Y. Zhu, W. Zhang, Reversible tuning of pore size and CO₂ adsorption in azobenzene functionalized porous organic polymers, Chem. Sci. 5 (2014) 4957–4961.
- [67] M. Frasconi, F. Mazzei, Electrochemically controlled assembly and logic gates operations of gold nanoparticle arrays, Langmuir 28 (2012) 3322–3331.
- [68] E. Kizilkan, J. Strueben, A. Staubitz, S.N. Gorb, Bioinspired photocontrollable microstructured transport device, Sci. Robot. 2 (2017) eaak9454.
- [69] R. Klajn, Immobilized azobenzenes for the construction of photoresponsive materials, Pure Appl. Chem. 82 (2010) 2247–2279.
- [70] L.M. Siewierski, W.J. Brittain, S. Petrash, M.D. Foster, Photoresponsive monolayers containing in-chain azobenzene, Langmuir 12 (1996) 5838–5844.
- [71] S. Sortino, S. Petralia, S. Conoci, S. Di Bella, Monitoring photoswitching of azobenzene-based self-assembled monolayers on ultrathin platinum films by UV/Vis spectroscopy in the transmission mode, J. Mater. Chem. 14 (2004) 811–813.
- [72] N. Delorme, J.F. Bardeau, A. Bulou, F. Poncin-Epaillard, Azobenzene-containing monolayer with photoswitchable wettability, Langmuir 21 (2005) 12278–12282.